

BLUR ESTIMATION IN LIMITED-CONTROL ENVIRONMENTS

Jeffery R. Price Timothy F. Gee Kenneth W. Tobin, Jr.

Image Science and Machine Vision Group
Oak Ridge National Laboratory
Oak Ridge, TN 37831-6010
{pricejr, geetf, tobinkwjr}@ornl.gov

ABSTRACT

In this paper, we propose a method to estimate the blur of a fixed imaging system, without control of camera position or lighting, using an inexpensive target. Such a method is applicable, for example, in the restoration of surveillance imagery where the imaging system is available, but with only limited-control of the imaging conditions. We extend a previously proposed parametric blur model and maximum likelihood technique to estimate a more general family of blur functions. The requirements for an appropriate characterization target are also discussed. Experimental results with artificial and real data are presented to validate the proposed approach.

1. INTRODUCTION

Image restoration [1] is the process of estimating an image from an observation that has undergone some degradation such as blur and/or additive noise. To perform any sort of image restoration, knowledge of the degradation or blur is required. Knowledge of the blur can be obtained in at least two ways, which we refer to as *blind* estimation and *perfect-control* estimation. In the blind estimation scenario [2, 3, 4], the blur is estimated directly from the degraded image(s). In the perfect-control setting, the imaging system used to capture the given image is characterized through some experimental process. This option, of course, is often infeasible or impractical. Obviously the imaging system cannot be subjected to a characterization process if it is unavailable and/or unknown. Even if the imaging system is available, however, current methods for characterization [5, 6] are often impractical as they require expensive targets, nearly ideal lighting, control of camera and/or target placement, and analysis by a skilled individual. These two alternatives – blind and perfect-control – represent two extremes of the blur estimation problem.

In this paper, we begin the investigation of a new technique for estimating image blur in *limited-control* environments. The limited-control environment falls between the two aforementioned extremes and is useful in surveillance and/or video forensics applications [7]. In such applications, an event of interest may be recorded by a fixed imaging system, such as a surveillance camera, that is available for limited testing in its native environment. As it may be desirable to improve the recorded image(s) using image restoration techniques, the goal of the work presented here is a robust method to estimate the blur of a fixed imaging system, without control of camera position or lighting, using an inexpensive target (or targets). Such a method is the primary contribution of this paper. Additionally, we extend the blur models and maximum likelihood estimation technique suggested in [2] to allow for a broader class of parametric blur functions.

The remainder of this paper is organized as follows. In Section 2, we present the parametric blur model, based upon that in [2], that we have adopted for our work. In Section 3, we discuss the maximum likelihood estimation of the blur parameters and then, in Section 4, we describe briefly the requirements for the characterization target. We present some experimental results from artificial and real data in Section 5 and make some closing comments in Section 6.

2. BLUR MODEL

In general, the blur of an optical imaging system can be very difficult to model. An accurate blur model based upon physical optics requires such parameters as depth of the imaged objects, lens aberrations, and spectral distribution of the incident light [8]. A more tractable approach is to employ parametric blur models based upon geometric or diffraction-limited assumptions. Such an approach is suggested in [8] as a reasonable alternative to the more cumbersome physical optics model and has been used successfully in the image processing literature [2, 9].

We adopt the continuous spatial domain approach presented by Pavlović and Tekalp in [2] with some modifica-

Work funded by the U.S. Department of Energy's Office of Nonproliferation Research and Engineering (NN-20).

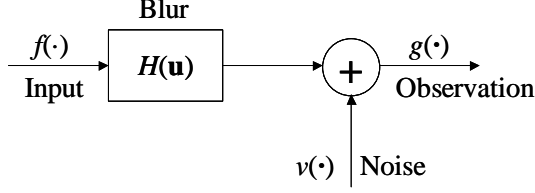


Fig. 1. Simple model of imaging system assuming linear, shift-invariant blur and additive noise.

tions and extensions. Specifically, in [2] out-of-focus circular aperture blur and circularly symmetric Gaussian blur are considered independently. We, however, allow for separable, elliptically symmetric Gaussian blur and additionally consider both out-of-focus and Gaussian blur simultaneously. The Gaussian is used to approximate any blur in the scene that may arise from sources other than focus error. We adopt the separable Gaussian because some imaging systems tend to have more blur in one direction than the other (e.g., the real data mentioned in Section 5). The point spread function (PSF) for the out-of-focus circular aperture is given by

$$h_c(\mathbf{x}; R) = \frac{1}{\pi R^2} \Pi_R(|\mathbf{x}|) \quad (1)$$

where

$$\Pi_R(|\mathbf{x}|) = \begin{cases} 1, & |\mathbf{x}| \leq R, \\ 0, & |\mathbf{x}| > R. \end{cases} \quad (2)$$

The PSF for the elliptically symmetric, separable Gaussian is

$$h_g(\mathbf{x}; \gamma_1, \gamma_2) = \frac{1}{2\pi\gamma_1\gamma_2} \exp\left(\frac{-x_1^2}{2\gamma_1^2}\right) \exp\left(\frac{-x_2^2}{2\gamma_2^2}\right) \quad (3)$$

The blur for the overall imaging system is given by the convolution of (1) and (3):

$$h(\mathbf{x}; R, \gamma_1, \gamma_2) = h_c(\mathbf{x}; R) * h_g(\mathbf{x}; \gamma_1, \gamma_2). \quad (4)$$

Letting θ represent the collection of blur parameters to be estimated, $\{R, \gamma_1, \gamma_2\}$, we can rewrite (4) in the Fourier domain as

$$H(\mathbf{u}; \theta) = \frac{1}{\pi R|\mathbf{u}|} J_1(2\pi R|\mathbf{u}|) \cdot \exp(-2\pi^2\gamma_1^2 u_1^2) \exp(-2\pi^2\gamma_2^2 u_2^2) \quad (5)$$

where $J_k(\cdot)$ is the k^{th} -order Bessel function of the first kind. Given the model of (5), the goal of blur estimation is then to estimate the parameters R , γ_1 , and γ_2 .

3. PARAMETER ESTIMATION

Referring to the imaging system model in Fig. 1, the input, $f(\mathbf{x})$, is characterized in [2] by an autoregressive model

driven by Gaussian-distributed, white noise. As we have some control over the input to the imaging system in the limited-control environment, we can simplify further and assume that the input is purely Gaussian noise with unknown variance σ_f^2 . Such an input can be approximated using a prefabricated target, as discussed in Section 4 below. The term $v(\cdot)$ represents additive white noise of unknown variance σ_v^2 . We let $g(\mathbf{n})$ represent the $N \times N$ observed samples of the image $g(\mathbf{x})$. Using the well-known block circulant approximation [10] to the covariance matrix of $g(\mathbf{n})$ (lexicographically ordered), and following the form of [2], the maximum likelihood parameters θ can be found by minimizing the negative of the likelihood function (LF)

$$L(\theta, \sigma_f^2, \sigma_v^2) = \sum_{\mathbf{k}} \log(S_g(\mathbf{k}; \theta)) + \frac{1}{N^2} \frac{|G(\mathbf{k})|^2}{S_g(\mathbf{k}; \theta)}, \quad (6)$$

where $S_g(\mathbf{k}; \theta)$ represents samples of the (analytically computed) power spectrum of $g(\mathbf{x})$ and where $G(\mathbf{k})$ is the discrete Fourier transform (DFT) of $g(\mathbf{n})$. Recalling that the input $f(\cdot)$ in Fig. 1 is purely white noise, we can write

$$S_g(\mathbf{u}; \theta) = \sigma_f^2 |H(\mathbf{u}; \theta)|^2 + \sigma_v^2 \quad (7)$$

where $H(\mathbf{u}; \theta)$ was given in (5). We note that $|H(\cdot)|^2 = H^2(\cdot)$ since $H(\cdot)$ is purely real.

To minimize (6) effectively, we must compute the gradients of $L(\cdot)$ with respect to each of the unknowns. Recalling that $\theta = \{R, \gamma_1, \gamma_2\}$, we have

$$\frac{\partial L(\cdot)}{\partial \theta_i} = \sum_{\mathbf{k}} \left(\frac{1}{S_g(\mathbf{k}; \theta)} - \frac{1}{N^2} \frac{|G(\mathbf{k})|^2}{S_g^2(\mathbf{k}; \theta)} \right) \cdot 2\sigma_f^2 H(\mathbf{k}; \theta) \frac{\partial H(\mathbf{k}; \theta)}{\partial \theta_i}, \quad (8)$$

for the blur parameters and

$$\frac{\partial L(\cdot)}{\partial \sigma_f^2} = \sum_{\mathbf{k}} \left(\frac{1}{S_g(\mathbf{k}; \theta)} - \frac{1}{N^2} \frac{|G(\mathbf{k})|^2}{S_g^2(\mathbf{k}; \theta)} \right) H^2(\mathbf{k}; \theta), \quad (9)$$

and

$$\frac{\partial L(\cdot)}{\partial \sigma_v^2} = \sum_{\mathbf{k}} \left(\frac{1}{S_g(\mathbf{k}; \theta)} - \frac{1}{N^2} \frac{|G(\mathbf{k})|^2}{S_g^2(\mathbf{k}; \theta)} \right) \quad (10)$$

for the signal and noise power, respectively. To complete (8), we must evaluate the partials of $H(\cdot)$ with respect to each of the blur parameters, yielding

$$\frac{\partial H(\cdot)}{\partial R} = \frac{1}{R} \exp(-2\pi^2\gamma_1^2 u_1^2) \exp(-2\pi^2\gamma_2^2 u_2^2) \cdot \left(J_0(2\pi R|\mathbf{u}|) - J_2(2\pi R|\mathbf{u}|) - \frac{1}{\pi R|\mathbf{u}|} J_2(2\pi R|\mathbf{u}|) \right) \quad (11)$$

and

$$\frac{\partial H(\cdot)}{\partial \gamma_i} = \frac{J_1(2\pi R|\mathbf{u}|)}{\pi R|\mathbf{u}|} \cdot \left(-2\pi^2 \gamma_i u_i^2 \exp(-2\pi^2 \gamma_1^2 u_1^2) \exp(-2\pi^2 \gamma_2^2 u_2^2) \right) \quad (12)$$

for $i = 1, 2$.

Given the DFT of the observed digital image, $G(\mathbf{k})$, the likelihood function $L(\cdot)$ from (6) is minimized with respect to the five unknown parameters – R , γ_1 , γ_2 , σ_f^2 , and σ_v^2 – using a constrained nonlinear minimization routine (the `fmincon` function from MATLAB’s Optimization Toolbox). Initial experimental results indicated some sensitivity to initial conditions, so a two-step initialization procedure is performed. In the first step, initial guesses for σ_f^2 and σ_v^2 are computed. In the second step, these initial guesses are used to compute $L(\cdot)$ over a 5×5 grid of equally spaced points (over the range of expected/allowable values, noted below) by assuming that $\gamma_1 = \gamma_2$. The minimizer over this 25 point set is then selected as the starting point for the optimization.

To constrain the optimization, the unknown parameters are allowed to take values in the following ranges: $R \in (0, 20]$, $\{\gamma_1, \gamma_2\} \in (0, 20]$, and $\{\sigma_f^2, \sigma_v^2\} \in (0, \infty)$. The allowable blur parameter (R, γ_1, γ_2) ranges are representative of what is reasonably expected in our application of interest.

4. CHARACTERIZATION TARGET

As mentioned at the beginning of the previous section, the goal of the target is to provide white, Gaussian-distributed noise as input to the imaging system. White noise ensures that the power spectrum $S_g(\cdot)$ takes the form of (7). The Gaussian distribution is required to satisfy the assumptions used to generate the likelihood function of (6).

The target we employ is composed of constant intensity blocks, where the intensity of each block is selected from a discrete, approximately Gaussian distribution over $[0.0, 1.0]$ (0.0 corresponds to black, 1.0 corresponds to white). In the ideal scenario, each block on the target would correspond to one pixel, with no overlap. Obviously, such a scenario would be quite difficult to ensure. Instead, we only require that the area of each target block correspond to less than the area of one pixel. In this situation there will be some correlation because adjacent pixels will generally be observing portions of some of the same target blocks. This correlation, however, is limited to a 3×3 window and is essentially negligible (in fact, it can be assumed to arise from blur and will therefore be modeled by the blur estimation).

We note that decreasing the area of each target block with respect to the area of each pixel would decrease the aforementioned correlation, but would also tend to decrease the effective SNR. As the number of target blocks observed by each pixel increases, the effective spread of $f(\cdot)$ about

its mean (i.e., σ_f^2) decreases. Therefore, we would like the target blocks to be smaller than, but on the same order of, the area imaged by each pixel. This can be accomplished in the field by having several targets with varying block sizes available. Finally, to account for illumination variations and nonlinear contrast modifications, we include a uniform gray bar and a black-to-white gradient bar, one each in both the horizontal and vertical directions, on the target image. The uniform gray bars are used to estimate and correct any illumination profile and the gradient bars are used to estimate and correct nonlinear contrast modifications.

5. EXPERIMENTAL RESULTS

In this section, we present experimental results from both artificial and real data. Artificial data was generated by first creating a Gaussian white noise image with known variance, σ_f^2 , of size 128×128 pixels. This noise image was then blurred by a PSF – obeying the model presented in Section 2 – with known parameters $\{R, \gamma_1, \gamma_2\}$. Gaussian, white noise with known variance σ_v^2 was then added to the blurred image to simulate the observation noise. The DFT of the noisy, blurred image was then used as $G(\mathbf{k})$ in (6). Real data was obtained using a consumer video camera, a PC with video capture capabilities, and a noise target such as that described in Section 4. To provide blurry images, the autofocus feature of the camera was disabled and the camera was manually defocused by varying degrees. The DFT of one captured frame was then used as $G(\mathbf{k})$ in (6). The real images, shown in Fig. 2, were (arbitrarily) scaled so that the initial guess for σ_f^2 was 10.0.

Some results obtained from the artificial data are summarized in Table 1. The algorithm performed similarly with various blur parameters. It should be evident from Table 1 that the algorithm performs quite well, even down to SNRs as low as 20dB. Around 15dB and less, the algorithm is not robust. This, however, has not been a significant limitation in our application.

In Table 2, we summarize results obtained from the real data. Although the good results obtained from the artificial data give confidence in the results from the real data, we also performed an additional subjective test. The blurs estimated from the defocused images were applied to images obtained using autofocus. The resulting, digitally blurred images corresponded well to the same images obtained with optical blurring by manual defocus. This indicates, albeit subjectively, that the estimated blur is representative of the true, optical blur. Ongoing work is aimed at quantifying more conclusively the accuracy and consistency of these results.

We now make a few comments regarding the data from Table 2. First we recall that each real image was scaled so that the initial guess for σ_f^2 was 10.0, hence the variation of the σ_f^2 estimates. For the “Small Defocus” results, we

	R	γ_1	γ_2	σ_f^2	σ_v^2
SNR 40dB					
True	6.2	0.9	1.8	10.0	0.001
Estimated	6.20	0.932	1.81	10.6	0.001
SNR 30dB					
True	6.2	0.9	1.8	10.0	0.01
Estimated	6.15	0.917	1.79	10.0	0.0102
SNR 20dB					
True	6.2	0.9	1.8	10.0	0.1
Estimated	6.21	0.961	1.91	11.4	0.101
SNR 15dB					
True	6.2	0.9	1.8	10.0	0.3162
Estimated	6.94	0.764	1.63	11.6	0.321

Table 1. Some results for artificial images. SNR is given by $10 \log_{10}(\sigma_f^2/\sigma_v^2)$.

	R	γ_1	γ_2	σ_f^2	σ_v^2
Autofocus	1.18	0.34	0.36	6.04	0.058
Small Defocus	1.46	1.60	3.58	7.43	0.067
Large Defocus	18.7	2.17	2.42	8.69	0.070

Table 2. Results for the real data shown in Fig. 2.

note that the Gaussian blur parameters indicate more blur in the x_2 (horizontal) direction than in the x_1 (vertical) direction. This result, although unexpected, was consistent with the observed image DFT, which indicated a stronger lowpass nature in the horizontal direction. This characteristic was not evident when autofocus was enabled or for the large defocus.

6. CONCLUSION

In this paper, we present a method to estimate the blur of a given imaging system in a limited-control environment using a noise target. A previously proposed blur model and maximum likelihood approach are extended to handle a more flexible class blur functions. We also discuss the requirements for constructing a suitable characterization target. Results from artificial and real data are given and demonstrate the performance of the proposed approach.

7. REFERENCES

[1] M.R. Banham and A.K. Katsaggelos, "Digital image restoration," *IEEE Signal Processing Mag.*, vol. 14, no. 2, pp. 24–41, March 1997.

[2] G. Pavlović and A.M. Tekalp, "Maximum likelihood parametric blur identification based on a continuous

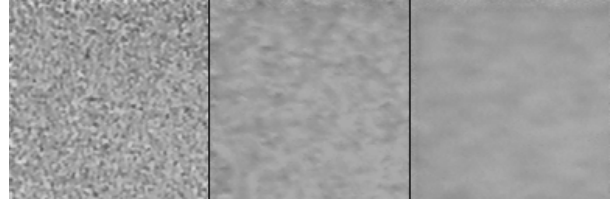


Fig. 2. Real data used for experiments summarized in Table 2. Autofocus, small defocus, and large defocus are shown from left to right.

spatial domain model," *IEEE Trans. on Image Processing*, vol. 1, no. 4, pp. 496–504, October 1992.

- [3] R.L. Lagendijk, J. Biemond, and D.E. Boeke, "Identification and restoration of noisy blurred images using the expectation-maximization algorithm," *IEEE Trans. on Acoustics, Speech, and Signal Processing*, vol. 38, no. 7, pp. 1180–1191, July 1990.
- [4] A.M. Tekalp, H. Kaufman, and J.W. Woods, "Identification of image and blur parameters for the restoration of noncausal blurs," *IEEE Trans. on Acoustics, Speech, and Signal Processing*, vol. 34, no. 4, pp. 963–972, August 1986.
- [5] International Standards Organization, *ISO 12233: 2000, Photography – Electronic Still-picture Cameras – Resolution Measurements*, ISO, 2000.
- [6] IEEE Broadcast Technology Society, *IEEE Std 208-1995, IEEE Standard on Video Techniques: Measurement of Resolution of Camera Systems, 1993 Techniques*, IEEE, 1995.
- [7] *IEEE Workshop on Visual Surveillance*, 2000.
- [8] H.-C. Lee, "Review of image-blur models in photographic system using the principles of optics," *Opt. Eng.*, vol. 29, no. 5, pp. 405–421, May 1990.
- [9] A.E. Savakis and H.J. Trussell, "Blur identification by residual spectral matching," *IEEE Trans. on Image Processing*, vol. 2, no. 2, pp. 141–151, April 1993.
- [10] R.L. Lagendijk, A.M. Tekalp, and J. Biemond, "Maximum likelihood image and blur identification: A unifying approach," *Opt. Eng.*, vol. 29, no. 5, pp. 422–435, May 1990.